

TWO CLASSES OF SOLAR PROTON EVENTS DERIVED FROM ONSET TIME ANALYSIS

SÄM KRUCKER AND R. P. LIN

Space Sciences Laboratory, University of California, Berkeley, Berkeley, CA 94720-7450; krucker@ssl.berkeley.edu

Received 2000 July 13; accepted 2000 August 18; published 2000 September 21

ABSTRACT

We analyze onset times for 26 solar energetic (from 30 keV to 6 MeV) proton events that exhibit clear velocity dispersion, as observed by the three-dimensional Plasma and Energetic Particles experiment on the *Wind* spacecraft. Assuming that the particles are injected simultaneously at all energies and travel the same path length, we find two classes of proton events: (1) for the 18 class 1 events, the derived path lengths are between 1.1 and 1.3 AU, indicating that the first arriving protons travel essentially scatter-free; and (2) the eight class 2 events show longer path lengths around 2 AU. For all proton events, the observed temporally related electron events all have electron path lengths around 1.1–1.3 AU. Relative to the electron injection time at the Sun, the protons of the first class are injected ~ 0.5 –2 hr later. Assuming these particles are accelerated by the associated coronal mass ejection (CME) shock, the protons at all energies between 0.03 and 6 MeV appear to be accelerated (or released) simultaneously high in the corona, roughly ~ 1 –10 R_{\odot} above the electrons. The pitch-angle distributions are observed to be similar for both classes of events, making it unlikely that propagation effects are responsible for the longer path length of class 2 events. The late proton onset times at 1 AU of class 2 are therefore more likely explained by a successively later solar release (or escape) of protons at successive lower energies. Assuming again acceleration at the CME shock, the release (or escape) of the protons of class 2 events appears to depend on energy and occur at a higher altitude for lower energies, with the most energetic protons possibly released simultaneously with the electrons.

Subject headings: acceleration of particles — interplanetary medium — Sun: flares — Sun: particle emission

1. INTRODUCTION

Solar energetic particle (SEP) events observed in interplanetary space near 1 AU generally show velocity dispersion in their onsets, indicating they are the result of sudden transient acceleration near the Sun. Two main classes of SEP events are distinguished (e.g., Reames 1999). “Impulsive” SEP events (so called because of the short [< 1 hr] duration of the associated soft X-ray [SXR] burst) are electron-rich and ^3He -rich and show high ionic charge states. They occur frequently ($\sim 10^3 \text{ yr}^{-1}$ over the whole Sun during solar maximum), and their escape is general restricted to a relatively small longitudinal cone ($< 50^\circ$). “Gradual” SEP events (e.g., with a long [> 1 hr] duration SXR burst) occur much less frequently (several tens per year at maximum), are proton-rich, and show normal coronal abundance and charge states corresponding to typical quiet coronal temperatures. They are typically observed over a large longitudinal cone ($\approx 180^\circ$) and are almost always related to a fast coronal mass ejection (CME).

Kahler (1994) analyzed greater than 10 MeV proton onset times and concluded that the proton release near the Sun occurs not earlier than the maximum of the flare impulsive phase and that the peak of the injection profile occurs when the associated CME reaches heights of 5–15 R_{\odot} . Electron release is observed to temporally coincide with the occurrence of radio type III bursts starting in the corona and traveling along open field lines into interplanetary space (see Lin 1985). Recent electron onset time analysis (Bothmer et al. 1997; Krucker et al. 1999) shows evidence that some electron events are not related to type III bursts. These tend to be proton-rich (i.e., gradual SEPs) and the electron release is observed to occur up to half an hour after the type III burst. Krucker et al. (1999) found that the electron release appeared related to the passage of large-scale coronal transient waves, also called EIT waves (Thompson et al. 1998, 2000), over the footpoint of the field line connected to the spacecraft. Torsti et al. (1999a, 1999b) suggested that

EIT waves might also be related to the release of 1–50 MeV protons.

In the present work, a survey of SEP events observed by the three-dimensional Plasma and Energetic Particles (3DP) instrument on the *Wind* spacecraft (Lin et al. 1995) is presented.¹ The timing of proton onsets in the energy range from ~ 30 keV to 6 MeV is investigated and compared to the release of 1–300 keV electrons. Two different classes of proton events could be distinguished.

2. OBSERVATIONS

In 3DP, six double-ended spectroscopic survey telescopes (SSTs), each with a pair or triplet of closely stacked silicon semiconductor detectors, provide full three-dimensional coverage with $36^\circ \times 22.5^\circ$ angular resolution for ~ 20 –400 keV electrons and ions from ~ 30 keV to 6 MeV. One end of each SST is covered with a Lexan foil (foil SST), which stops protons up to ~ 400 keV while ≥ 20 keV electrons are essentially unaffected. The opposite end is open (open SST) but has a magnet that sweeps away electrons below ~ 400 keV while leaving the ions unaffected. Thus, when no higher energy particles are present, electrons and ions below ~ 400 keV are cleanly separated. Most electrons above ~ 400 keV will penetrate the front detector and be anticoincided by the rear detector. Protons from 400 keV to 6 MeV are measured by the open SST, and their contribution to the foil SST can be computed. Heavier ions such as He or CNO require higher energies to penetrate the foil. By comparing the response of the open and foil SSTs, some information on the ion species may be obtained. For some SEP events, such as 1997 November 4 and 6, 1998 April 20, etc., the associated greater than 400 keV electron flux is large enough to significantly contaminate the

¹ A list of *Wind* 3DP SEP events is available at <http://plasma2.ssl.berkeley.edu/~krucker>.

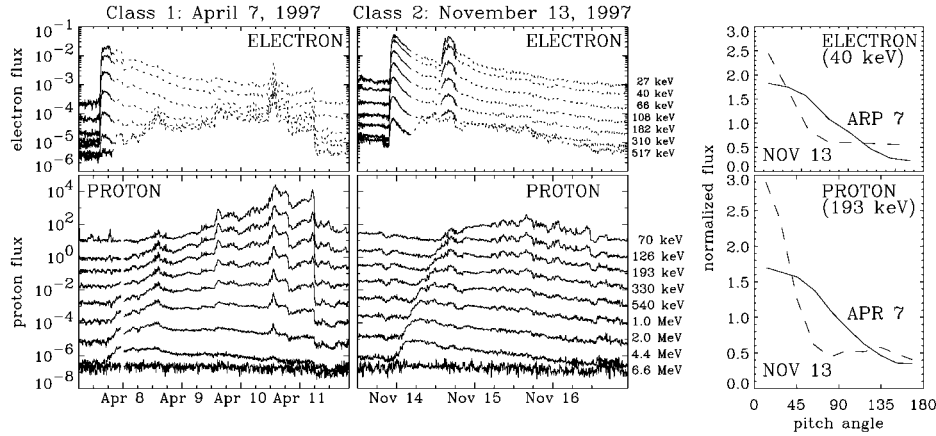


FIG. 1.—Overview plots of the SEP events on 1997 April 7 (*left*) and November 13 (*middle*). The top and bottom panels show the electron and proton fluxes around zero degree pitch angle ($<90^\circ$) at different energies as indicated. For a clearer representation, the proton curves are subsequently offset by a factor of 4.4 starting at the highest energy. The dotted curves in the electron plots indicate times when protons are contaminating the foil SST detectors. On the right, the pitch-angle distributions for 30–50 keV electrons (*top*) and 115–279 keV protons (*bottom*) are presented. The shown fluxes are over the first hours of the events averaged values normalized by the pitch-angle averaged flux.

open SSTs. These events ($\sim 50\%$ of the total number of events) are therefore not included in the present survey. Electrostatic analyzers in 3DP provide measurements of solar wind and suprathermal electrons and ions up to ~ 30 keV.

Two examples of SEP events with velocity dispersion are presented in Figure 1. The pitch-angle distributions (Fig. 1, *right*) show that electrons as well as ions are collimated along the magnetic field lines. There is a second electron event occurring after 13 UT on 1997 November 14, which is not discussed in this Letter, and the spike in the ion flux on 1997 April 10 is related to an interplanetary shock crossing the spacecraft.

The arrival time at 1 AU, $t_{1\text{AU}}(E)$, of a particle with energy E is given by

$$t_{1\text{AU}}(E) = t_{\text{Sun}}(E) + L(E)v^{-1}(E), \quad (1)$$

where $t_{\text{Sun}}(E)$ is the particle release time at the Sun, $v(E)$ is the velocity, and $L(E)$ is the path length. If particles at all energies are released simultaneously and travel the same path length, the observed arrival times $t_{1\text{AU}}(E)$ would be a linear function of $v^{-1}(E)$ with a slope equal to the (constant) path length L and an intersection at $v^{-1} = 0$ equal to t_{Sun} . The onset times at different energies are determined by eye and are plotted in Figure 2 versus $\beta^{-1} = c/v$, where the origin of the time axis corresponds to the onset time of the radio type III burst at the Sun. The error bars shown are a very conservative bracketing of the onset times: before these time periods, the event definitely has not yet started, and afterward the flux is already clearly increased above the background (cf. Krucker et al. 1999).

Out of a total of 26 events, 18 are of the type shown on the left in Figure 2 (denoted class 1). The linear fits show the same

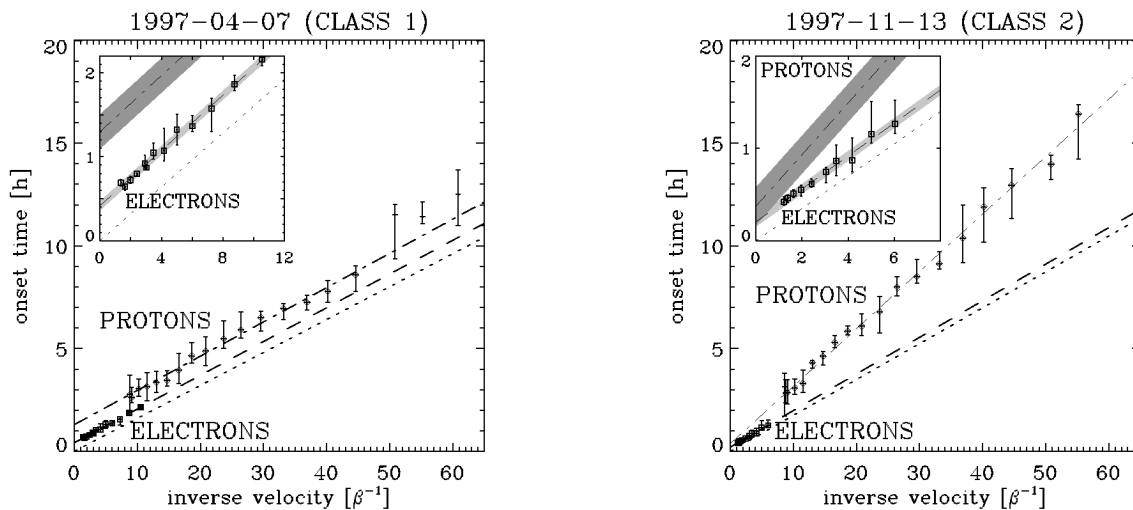


FIG. 2.—Comparison of proton (*diamonds*) and electron (*squares*) onset times at 1 AU for the two events discussed in this Letter. The onset time after the radio type III burst onset at the Sun as a function of the inverse velocity is shown. The dashed-dotted and dashed lines are linear fits to the proton and electron onset times, respectively. The dotted lines show the expected onset times at 1 AU for particles traveling scatter-free along the Parker spiral assuming they are released at the time of the radio type III burst onset at the Sun. The inserts show a close-up of the same plots for a clearer representation of the electron onset times. The shaded areas represent the uncertainties in the fitted curves.

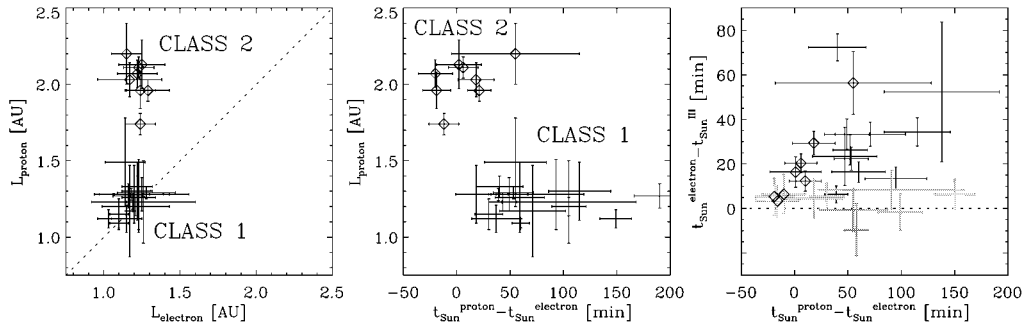


FIG. 3.—Statistical results. (Left) The path lengths derived from the proton onset L_{proton} are compared with the path lengths derived from the electron onset L_{electron} . (Middle) The delay between the proton and electron release times at the Sun, $t_{p, \text{Sun}} - t_{e, \text{Sun}}$ are plotted against L_{proton} . (Right) The electron release times relative to the type III burst onsets are shown as a function of $t_{p, \text{Sun}} - t_{e, \text{Sun}}$. Events for which the electron release is simultaneously with the type III onset are shown in gray. In all plots, class 2 events ($L_{\text{proton}} > L_{\text{electron}}$) are marked with diamonds.

slope for protons (dash-dotted line) and electrons (dashed line), indicating that the first arriving protons and electrons are traveling about the same distance ($L_p = 1.20 \pm 0.05$ AU and $L_e = 1.19 \pm 0.04$ AU), a path length comparable to the Parker spiral length of 1.16 AU calculated from the averaged observed solar wind speed for this day. The intersections of the fitted lines with the vertical axis give the solar release time of the electrons, $t_{\text{Sun}} \approx 14:19 \pm 3$ UT, i.e., 26 ± 5 minutes after the type III onset at the Sun (chosen as $t = 0$), and the first protons appear to be released an additional 54 ± 12 minutes later than the first electrons.

The second type of event (class 2) is shown on the right in Figure 2. The electron onset times give again a path length ($L_e = 1.29 \pm 0.13$ AU) comparable to the Parker spiral length (1.26 AU), but the protons appear to travel a much longer distance ($L_p = 2.02 \pm 0.07$ AU). Contrary to the previously presented event, the solar release times of protons ($21:36 \pm 12$ UT) and the electrons ($21:26 \pm 3$ UT) are simultaneous within the uncertainties. For this event, $t_{e, \text{Sun}}$ is still significantly delayed by 12 ± 3 minutes compared to the type III radio burst onset ($\sim 21:14$ UT).

Figure 3 (left) compares the derived path lengths for protons and electrons for the 26 analyzed events. For class 1 (18 events), the electrons and protons have similar path lengths of about the Parker spiral field length, and for class 2 (eight events), the protons have a significantly larger path length (~ 2 AU). In class 1 events ($L_p \approx L_e$), the proton release times are delayed relative to electrons by about 1 hr, whereas for class 2 ($L_p > L_e$), protons and electrons seem to be released simultaneously within the uncertainties of about 20 minutes (Fig. 3, middle).

The two classes of proton events do not correspond to the two classes of electron events reported by Krucker et al. (1999). They found that the release times of one class of electron events occur simultaneously with the radio type III burst onsets, whereas the release time of the other class of events is later than the type III burst onset. Figure 3 (right) shows that for class 1 events, seven out of 18 of the related electron events are released simultaneously with the type III burst onset, and for class 2, three out of eight events are released simultaneously, within the accuracy of roughly ± 8 minutes. As also reported by Krucker et al. (1999), the associated SXR flare locations of type III associated electron events occur on a narrower range of longitudes (with a standard deviation of $\sim 30^\circ$) than for the related events that are not type III (45°).

3. DISCUSSION

For the 26 events analyzed (1) 21 events have a *GOES* SXR flare, three with a possible SXR flare; (2) 17 events have a coronal type III burst (Solar Geophysical Data);² (3) all 26 events have an interplanetary type III burst (*Wind WAVES*); and (4) 15 events have a coronal type II burst (Solar Geophysical Data).² All 16 events with the *Solar and Heliospheric Observatory (SOHO)* large-angle spectrometric coronagraph (*LASCO*) coverage show an associated CME. A detailed temporal comparison with the derived particle release times, however, does not show any obvious correlation of a particular type of associated solar event with the two classes of events presented above. Further correlation studies including flare locations, pitch-angle distributions, and proton spectra also do not show any obvious correlation between the two classes of proton events.

In class 1 events the first arriving electrons and protons both travel about the Parker spiral field line length, so the delay of the protons relative to the electrons most likely is due to a delayed release near the Sun. When the spacecraft is magnetically well connected to the flare site, the type III producing electrons are detected and the electron release time coincides with the type III onset time. If the spacecraft is not magnetically well connected to the flare site, the only electrons detected are those related to the EIT wave (probably shock-accelerated; see Krucker et al. 1999), resulting in the delayed release time relative to the type III onset. At the time of the proton release of class 1 events, the SXR flare, impulsive radio bursts, etc., are over, and the only ongoing solar event in most cases is the CME moving away from the Sun. Assuming the proton acceleration/release is related to the CME shock front (Kahler 1996), *LASCO* CME observations (A. Vourlidas 2000, private communication) suggest that this occurs when the CME reaches altitudes between 2 and $26 R_\odot$ with an average value around $10 R_\odot$. The earlier release times of electrons relative to protons suggest that electrons are released at lower altitude, ~ 1 to $\sim 10 R_\odot$ lower than the protons.

The much longer path lengths in class 2 events might be explained if the assumed “proton” fluxes are dominated by heavier ions (e.g., ^3He), which travel much slower than protons of the same total energy. However, the 392–646 keV foil SST

² See ftp://ftp.ngdc.noaa.gov/STP/SOLAR_DATA.

count rates during the proton event (see Fig. 1, *top*) are comparable to the 615–821 keV open SST count rates as expected for protons. Heavier ions require much higher energies to penetrate the foil (~ 850 keV for helium and 2.5 MeV for oxygen). Therefore, we can exclude the possibility that the observed ion time profiles at these energies are dominated by heavier ions. The ULEIS experiment on the *Advance Composition Explorer* spacecraft also show that the events presented in this work are dominated by protons (J. E. Mazur 2000, private communication). Also, the preevent backgrounds and peak-to-background ratios for class 1 and class 2 events are generally comparable; thus, class 2 events are not due to higher background masking the onsets.

Since the first arriving electrons travel essentially along the Parker spiral field line and the solar wind speed does not change significantly, it is very unlikely that the protons in class 2 events travel along different, much longer field lines. A longer path length would result, however, if the first arriving protons have suffered much more pitch-angle scattering than the electrons. However, the electron and proton pitch-angle distributions during the first hours after the onset are very similar, both collimated within $\sim 40^\circ$ of the field (Fig. 1, *right*). Furthermore, the class 2 event presented in Figure 1 is even better collimated than the essentially scatter-free propagating class 1 event. While these pitch-angle observations at 1 AU only provide information about scattering within a few tenths of an AU, it appears unlikely that strong proton pitch-angle scattering is occurring in class 2 events; most likely, the proton path length is the same as for electrons. Then the observed monotonically longer delays at lower energies must result from a later acceleration or from a later escape of lower energy protons near the Sun.

Assuming the protons are accelerated by a CME shock, the onset times at lower energies would imply that the shock accelerates or releases the lower energy protons at higher altitudes only. For the event on November 13, ~ 6 MeV protons are re-

leased when the CME reaches heights around $\sim 5 R_\odot$, whereas ~ 0.3 MeV protons are released at about $\sim 12 R_\odot$. Preliminary analysis of proton onset times in the 25–53 MeV ($\beta^{-1} = 7.8\text{--}3.5$) range observed by the COSTEP experiment (Müller-Mellin et al. 1995) on *SOHO* show that the onset times also at semirelativistic energies follow the same trend as in the 0.1–6 MeV range (Fig. 2, *left*). Assuming that the first escaping 50 MeV particles travel essentially scatter-free along the Parker spiral, the solar release time of 53 MeV protons for the 1997 November 13 event would be $21:48 \pm 19$ UT compared to $21:26 \pm 3$ UT for the 9–300 keV electrons. Therefore, ~ 70 MeV protons might be released together with the electrons, whereas lower energies are accelerated-delayed or escape-delayed.

A delayed escape might be due to particle trapping or pitch-angle scattering near the Sun, which holds the protons back before they finally escape. Trapping can occur at a quasi-perpendicular shock (i.e., the angle θ between the shock normal and the magnetic field is close to 90°) as observed at the Earth's bow shock (Anderson et al. 1979) if the particle velocity normal to the shock is slower than the shock speed. A continuous decrease of θ away from the quasi-perpendicular value, which could occur as the shock moves away from the Sun, allows the escape of particles at successively lower energies.

We wish to thank all of the individuals who contributed to the success of the 3DP investigation on *Wind*: in particular, R. D. Campbell at the University of California, Berkeley, and T. R. Sanderson at ESTEC. We also thank R. P. Lepping at Goddard Space Flight Center for providing *Wind* MFI data and J.-L. Bougeret at the Paris Observatory for providing *Wind* WAVES data. This research is funded in part by NASA grants NAG5-2815 and NAG5-6928 at Berkeley. S. K. is also partially supported by the Swiss National Science Foundation (grant 8220-056558).

REFERENCES

- Anderson, K. A., et al. 1979, *Geophys. Res. Lett.*, 6(5), 401
 Bothmer, V., et al. 1997, in *Proc. 31st ESLAB Symp., Correlated Phenomena at the Sun, in the Heliosphere, and in Geospace*, ed. A. Wilson (ESA SP-415; Noordwijk: ESA), 207
 Kahler, S. W. 1994, *ApJ*, 428, 837
 ———. 1996, in *AIP Conf. Proc. 374, High Energy Solar Physics*, ed. R. Ramaty, N. Mandzhavidze, & X.-M. Hua (New York: AIP), 61
 Krucker, S., Larson, D. E., Lin, R. P., & Thompson, B. J. 1999, *ApJ*, 519, 864
 Lin, R. P. 1985, *Sol. Phys.*, 100, 537
 Lin, R. P., et al. 1995, *Space Sci. Rev.*, 71, 125
 Müller-Mellin, R., et al. 1995, *Sol. Phys.*, 162, 483
 Reames, D. V. 1999, *Space Sci. Rev.*, 90, 413
 Thompson, B. J., et al. 1998, *Geophys. Res. Lett.*, 25, 2461
 ———. 2000, *Sol. Phys.*, 193, 161
 Torsti, J., Kocharov, L. G., Teittinen, M., & Thompson, B. J. 1999a, *ApJ*, 510, 460
 Torsti, J., et al. 1999b, *J. Geophys. Res.*, 104, 9903